

Estimations of the muon content of cosmic ray air showers between 10 PeV and 1 EeV from KASCADE-Grande data

J.C. Arteaga-Velazquez^{a,*} for the KASCADE-Grande Collaboration

^a*Instituto de Física y Matemáticas, Universidad Michoacana,
Morelia, Mexico*

E-mail: juan.arteaga@umich.mx

Measurements of KASCADE-Grande on the muon size in high energy extensive air showers (EAS) have provided evidence that the actual attenuation length of shower muons in the atmosphere is larger than the expectations from the hadronic interaction models QGSJET-II-04, EPOS-LHC and SIBYLL 2.3. This discrepancy is related to a deficient description of the shower muon content with atmospheric depth by Monte Carlo (MC) models. To further explore the origin of the above anomaly, we have investigated the muon size as a function of the primary energy at different zenith angles using data from the KASCADE-Grande experiment. The procedure consisted in comparing the measured muon number flux against the predictions of a reference cosmic ray energy spectrum and from the observed difference to estimate the data/MC muon ratio that best describe the measurements. The ratio is then applied to the MC simulations and from here, we estimate the muon content versus the primary energy. As a reference model, we employed the energy spectrum measured from the Pierre Auger observatory, while, for the different cosmic ray abundances, the GSF model. Results are presented using the QGSJET-II-04, EPOS-LHC, SIBYLL 2.3 and SIBYLL 2.3c models in the analysis procedure.

*37th International Cosmic Ray Conference (ICRC 2021)
July 12th – 23rd, 2021
Online – Berlin, Germany*

*Presenter

1. Introduction

The analysis of the muon content in extensive air showers (EAS) with primary energies above 10 PeV from measurements of several experiments seems to reveal important discrepancies between the data and the predictions of modern high-energy hadronic interaction models [1], QGSJET-II-04 [2], EPOS-LHC[3] and SIBYLL 2.3 [4]. In particular, the studies point out an excess in the measured number of shower muons over expectations, which seems to increase with the primary energy. To investigate this anomaly with KASCADE-Grande [5], we have performed an analysis of the data from the experiment to estimate the muon content (N_μ) in cosmic-ray induced EAS as a function of the primary energy from 10^{16} eV to 10^{18} eV. Then, we compared these muon estimations with the predictions of the hadronic interaction models QGSJET-II-04, EPOS-LHC and SIBYLL 2.3 and SIBYLL 2.3c [6].

For this analysis, due to the lack of a model independent energy estimator in KASCADE-Grande, we have used the analysis method proposed by the NEVOD-DECOR [7, 8] and the SUGAR [9] cosmic-ray experiments. The idea is to compare the measured muon flux, $d\Phi_{exp}/dN_{\mu,exp}$, against another one, $d\Phi_{sim}/dN_{\mu,sim}$, predicted by a reference model for the energy and composition of cosmic rays. Then, from the difference between the fluxes, the ratio between the data and the MC muon number (R) that best describes the data is found based on the following equation [1]:

$$\begin{aligned} d\Phi_{exp}(N_{\mu,exp})/dN_{\mu,exp} &= d\Phi_{sim}(N_{\mu,sim})/dN_{\mu,sim} \times dN_{\mu,sim}/dN_{\mu,exp} \\ &= d\Phi_{sim}(N_{\mu,exp}/R)/dN_{\mu,sim} \times 1/R. \end{aligned} \quad (1)$$

Finally, by applying the R factor to the MC data, we estimate the measured muon number as a function of the energy. In the following sections, we will present the details of the experimental apparatus, the selected data, the Monte Carlo (MC) simulations, the method of analysis and the results. We will end with the corresponding conclusions.

2. The KASCADE-Grande detector and the measured data

KASCADE-Grande was a cosmic ray experiment located close to sea level (110 m a.s.l.) in the campus north of the Karlsruhe Institute of Technology (49.1° N, 8.4° E), Germany [5, 10]. It consisted of a complex of particle detectors aimed to measure the electromagnetic, muon and hadron components of EAS induced by cosmic rays with primary energies from 1 PeV up to 1 EeV. The experiment was conceived as a particle detector array formed by different types of detectors (a calorimeter, scintillator and muon detectors, multiwire proportional chambers, underground tracking detectors, and streamer tubes). KASCADE and Grande were the main detector systems of the experiment (see fig. 1). Shower electrons and photons (with threshold energy of 5 MeV for vertical incidence) were measured with the main array of KASCADE, which consisted of a 200×200 m² square grid of 252 liquid scintillator detectors spaced 13 m apart and grouped into 16 detector clusters. On the other hand, shower muons (with energies > 230 MeV for vertical incidence) were detected with a set of 192 shielded plastic scintillator detectors located under the electromagnetic detector units belonging to the outer clusters of the KASCADE array. Charged particles ($e + \mu$ with more than 3 MeV for vertical incidence) from air showers were registered with the Grande array, which was an hexagonal grid of 700×700 m² composed by 37 plastic scintillator

detectors (divided into 18 hexagonal clusters) separated by a mean distance of 137 m from each other. Together, the shielded and unshielded detectors from KASCADE and the scintillator detectors from Grande provided measurements of the total number of shower electrons (N_e), muons (N_μ) and charged particles (N_{ch}) on an event-by-event basis. Grande also supplied measurements to estimate the shower core position and the shower axis direction.

KASCADE-Grande collected data from December 2003 to November 2012. In our analysis, we have used measurements from this period. In total, we analysed a subsample of 1.276×10^7 events corresponding to an effective time of 1.577×10^8 s. The data were selected after the application of a set of selections cuts, which were carefully chosen to diminish the impact of the systematic uncertainties in the present study.

The chosen data only include events that were successfully reconstructed and that were acquired during stable runs with no hardware problems and in which all the muon and electromagnetic KASCADE clusters were active. Runs with less than 18 active Grande clusters were also discarded. The data that we studied were collected for zenith angles $\theta < 40^\circ$. This selection avoids the introduction of systematic errors that increase with θ . We also used data with shower cores located in a central area of Grande with radial distances $r = [150 \text{ m}, 650 \text{ m}]$ from the center of KASCADE (c.f. fig. 1). This way, we reduced edge effects in our analysis. EAS with large uncertainties in the total shower size were removed from our data subsample by requiring events that triggered at least one of the Grande clusters, produced signals in more than 11 Grande stations, had shower ages between -0.385 and 1.485 and total shower sizes $N_\mu > 3 \times 10^4$ and $N_e > 1 \times 10^4$. The selected data satisfy also a final cut, which refers to the deposited energy in the Grande detectors. This criterion removes reconstructed EAS with large bias in N_{ch} , N_e and N_μ .

After selection cuts, the corresponding trigger and reconstruction energy threshold for cosmic ray events is $\log_{10}(E/\text{GeV}) = 7.1 \pm 0.2$, whereas the muon and charged particle number thresholds for EAS are $\log_{10}(N_\mu) = 5.15 \pm 0.15$ and $\log_{10}(N_{ch}) = 6.1 \pm 0.3$, respectively. The thresholds were estimated using MC data, which will be described in the next section.

3. MC simulations

To perform this analysis, we have produced a set of MC simulations using CORSIKA v7.5 [11] without thinning for five primary nuclei: H, He, C, Si and Fe. Here, we employed Fluka 2011.2 [12] to simulate hadronic interactions with $E_h \leq 200$ GeV and four different hadronic interaction models, QGSJET-II-04, EPOS-LHC, SIBYLL 2.3 and SIBYLL 2.3c, for the simulations at higher energies. The events were generated for $\theta < 42^\circ$ and inside the primary energy interval from 10^{15} eV to 3.16×10^{18} eV following an E^{-2} spectrum.

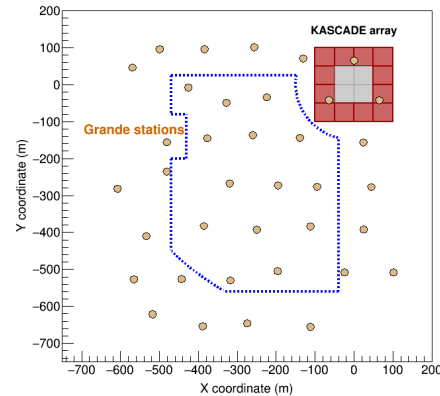


Figure 1: Diagram of the KASCADE-Grande layout. In the upper right corner, we observe the position of the KASCADE array. In red, we show the outer KASCADE clusters, and in gray the inner ones. The small circles indicate the position of the Grande detectors. The dotted line encloses the fiducial area used for the analysis in this work.

The QGSJET-II-04 data sets for each mass group were weighted in order to simulate power-law spectra with $\gamma = -3$ with the same intensity. They were combined to create a MC data set with a mixed composition scenario where all elements are present on equal abundances. These data were used to construct a muon correction function that was applied to the MC and the experimental data event-by-event following [13, 14] to reduce the systematic uncertainties in the estimated muon number.

On the other hand, by weighting the MC simulations for each high-energy hadronic interaction model, we have produced the reference energy and composition model of cosmic rays for our analysis. As a reference model we have used the total energy spectrum reported in [15] by the Pierre Auger Collaboration for $E \geq 3 \times 10^{17}$ eV, while, at lower energies, the spectrum predicted by the GSF model [16]. The latter was also used to describe the relative abundances of cosmic ray nuclei above 1 PeV. The GSF model provides the relative abundances for H, He, O and Fe primaries. However, as we do not have simulations for oxygen nuclei, we have used our MC data for carbon primaries instead. On the other hand, we did not incorporate the simulations for Si nuclei in our reference data sets. The energy spectra for the H, He, C and Fe mass groups in our reference model are plotted in fig. 2.

4. Analysis procedure

We divided the data sets into three zenith angle intervals with approximately the same aperture, i.e., $[0^\circ, 21.78^\circ]$, $[21.78^\circ, 31.66^\circ]$ and $[31.66^\circ, 40^\circ]$. For each of them, we built the histograms for the muon size (N_μ). The latter is carried out for our reference MC data sets and the experimental data. To create the muon histograms, we used data in the interval $\log_{10}(N_\mu) = [5.0, 7.4]$. For $\log_{10}(N_\mu) < 7.0$, we employed bins of size 0.2 and for $\log_{10}(N_\mu) = [7.0, 7.4]$, a single bin.

Then, in order to get insight into the dependence of the actual muon size in EAS with the primary energy, E , we compared the muon histograms for measured and MC data using a χ^2 -minimization procedure with MINUIT from ROOT [17], in particular, we look for the shift in $\log_{10}(N_\mu)$ that is needed to apply to the MC simulations as a function of the MC primary energy to reproduce the experimental muon histogram. We minimized the following quantity

$$\chi^2 = \sum_{i=1}^m \left(\frac{n_{exp,i} - n_{MC,i}}{\sigma_{i,MC}} \right)^2, \tag{2}$$

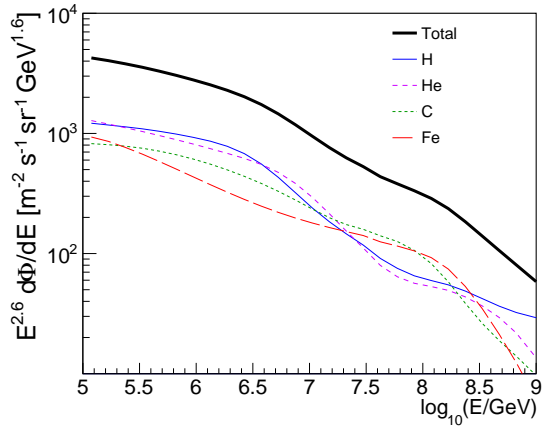


Figure 2: Cosmic ray energy spectra for the H, He, C and Fe mass groups in our reference model. The model is based on the GSF composition model [16] and the Pierre Auger total energy spectrum [15].

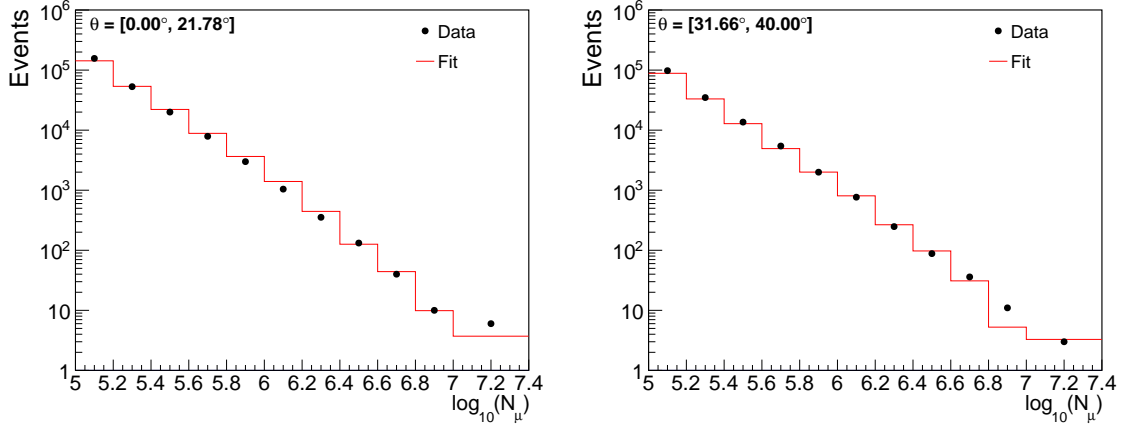


Figure 3: Histogram of the measured N_μ (black dots) and the result of the fit (red lines) using QGSJET-II-04 and the shift in MC data given by equation (3). Here, events with $\theta < 21.78^\circ$ (left) and $31.66^\circ < \theta < 40^\circ$ (right) were considered.

where $i = 1, \dots, m$ runs over each $\log_{10}(N_\mu)$ bin and $n_{exp,i}(n_{MC,i})$ is the measured (simulated) number of events for the i -th bin. On the other hand, $\sigma_{i,MC}$ is the expected error per bin, which is calculated using the square root of the sum of the square of weights inside the corresponding bin.

The shift in the muon number is parameterized as follows:

$$\delta_\mu = \Delta \log_{10}(N_\mu) = a_0 + a_1 \cdot \log_{10}(E/\text{GeV}) + a_2 \cdot \log_{10}^2(E/\text{GeV}). \quad (3)$$

Here, a_j ($j = 0, 1, 2$) represents the fitting parameters. The formula is fitted for the data in each zenith angle interval. As an example, the results of the fit of the measured data for vertical and inclined events are shown in fig. 3 using QGSJET-II-04.

We then applied the fitted shift, given by eq. 3, to the true N_μ of the corresponding MC simulations used for the analysis. This will be our estimated $N_\mu^{exp}(E)$ from the experimental data for the corresponding zenith angle interval. The analysis was performed using the four post-LHC high-energy hadronic interaction models considered in this work.

5. Results

For each zenith angle interval, and hadronic interaction model, we computed the estimated $\log_{10}[N_\mu/E(\text{GeV})]$ from the measured data as a function of the primary energy $\log_{10}(E/\text{GeV})$. We displayed the results in this form due to the narrow separation of the results in the $\log_{10}(N_\mu)$ vs $\log_{10}(E/\text{GeV})$ phase space. The plots are shown on the panels of fig. 4 and are compared with fits to the predictions of the post-LHC hadronic interaction models for H, Fe and our reference composition model. In each panel, the hadronic model used to estimate the muon content from the measured data is used to compute the expectations. The graphs are also plotted along with their respective statistical and systematic uncertainties.

As statistical error we provide the standard error on the mean added in quadrature with the statistical error due to the limited MC sample. On the other hand, the systematic error has different contributions, which were added in quadrature to obtain the total systematic uncertainty. The sources of systematic errors are listed below:

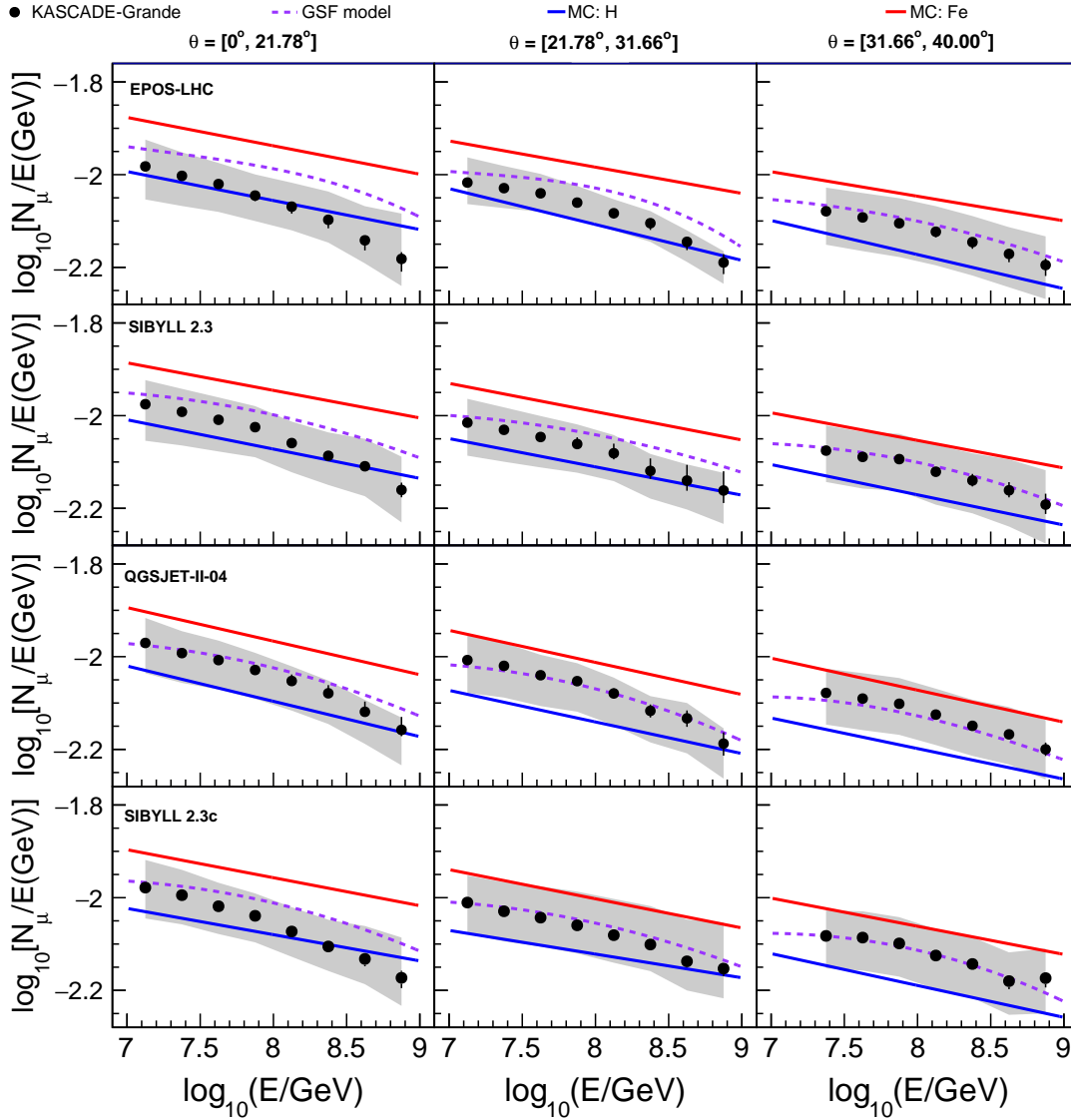


Figure 4: Experimental (data points) and expected (lines) mean values of $\log_{10}[N_\mu/E(\text{GeV})]$ versus $\log_{10}(E/\text{GeV})$ in the framework of several post-LHC hadronic interaction models, from top to bottom: EPOS-LHC, SIBYLL 2.3, QGSJET-II-04 and SIBYLL 2.3c. Each column correspond to a different zenith angle bin. Inside each panel, the upper red lines represent the expectations for Fe , the middle segmented lines in violet, for the GSF model and the lower blue lines, for H . The vertical error bars on the experimental plot represent statistical errors, while the gray band, the total systematic error.

- Error due to the shape of the energy spectrum: It was evaluated by employing the energy spectrum from the GSF model in the analysis instead of the Auger spectrum that we used as a reference for this study. The differences between the results obtained using both spectra were considered as the corresponding systematic error.
- Error due to uncertainties in composition: It was estimated by varying the relative abundance of the heavy (C+Fe) to the light (H+He) mass groups. For the GSF model, the ratio is close to 1.61 around $E = 100$ PeV. To calculate the corresponding systematic error on the muon

number, we modified the relative heavy/light abundance in our MC simulations in such a way that we have a ratio of 2.9 and another one with 0.99 at 100 PeV. These values are close to other ones observed from previous analyses of composition in KASCADE-Grande using different post-LHC hadronic interaction models (QGSJET-II-04, EPOS-LHC and SIBYLL 2.3) [18]. The maximum/minimum variations in the results with respect to the reference value were computed as the systematic uncertainties due to composition.

- Influence of uncertainties in the muon lateral distribution function (LDF): In previous works [14], we have observed that the actual lateral distribution functions of muons seems to be steeper than the expected from MC simulations. This difference seems to produce a systematic bias on N_μ which depends on the distance to the center of the array of muon detectors. To quantify the influence of this effect on the final result, we have divided the fiducial area in two regions, each of them with approximately the same acceptance. That was carried out by applying a radial cut at $r = 410$ m. Then, we calculated $\log_{10}[N_\mu/E(\text{GeV})]$ for each subsample and compared them with the standard result. The maximum and minimum differences were taken as the limits of the respective systematic errors.
- Uncertainty on the estimated fitted parameters: We computed this error by varying the fitted parameters, which are applied to the MC data, inside the corresponding 68 % C.L. intervals. The maximum range of variation of the muon content vs energy with that obtained from the reference value was registered as the corresponding systematic uncertainty.
- Uncertainty on the energy scale: The energy scale used in the spectrum of the Pierre Auger observatory has a conservative systematic error of ± 14 %. We have varied the energy scale by ± 14 % in our composition model and have repeated the calculations. For the upper energy limit, we got the smaller values for the estimated muon size from the data, and for the lowest one, the largest values of N_μ . The differences with respect to the reference value with no shift in the energy scale were taken as the systematic errors due to the uncertainty in the energy scale.

The total systematic errors are dominated by contributions from uncertainties in the energy calibration and the LDF of muons. The former is the largest one for all zenith angles. It is important to comment that the error due to the LDF of muons decreases for large zenith angles. For vertical events the differences are greater at high-energies as the actual muon LDF seems to be steeper than the one used to reconstruct the estimated N_μ size in MC simulations and even that the data itself in this energy regime [19].

From fig. 4, we observe that none of the high-energy hadronic interaction models studied here is able to describe consistently the total muon number of EAS measured in KASCADE-Grande at different zenith angles. In particular, we observe that the predictions of the EPOS-LHC, SIBYLL 2.3 and SIBYLL 2.3c do not contain the measurements of the KASCADE-Grande experiment for vertical EAS at high energies. Here, we observe that the actual data are below the MC simulations. On the other hand, the curves of $N_\mu(E)$ for MC and experimental data seem to be in better agreement for inclined EAS.

In addition, we notice that the data seem to imply that the composition of cosmic rays becomes heavier at higher zenith angles. Such behavior seems to be in agreement with another anomaly

reported in [14], which implies that the measured muon attenuation length is larger than in MC simulations.

It is interesting to note that for large zenith angles we are sampling the muon energy spectrum at production site for higher muon energies. Therefore, these anomalies may be correlated with differences in the muon energy spectra between measured data and model expectations. In this case, our results would imply that the muon energy spectra predicted by the post-LHC models are steeper than the corresponding ones for the measured data.

6. Conclusions

We have estimated the muon content of EAS versus the primary energy in actual EAS using KASCADE-Grande data for the range from $E = 10^{16}$ eV to $E = 10^{18}$ eV and zenith angles $\theta \leq 40^\circ$. The comparison with the predictions of the hadronic interaction models QGSJET-II-04, EPOS-LHC, SIBYLL 2.3 and SIBYLL 2.3c reveals several differences between the muon data and the models, which could imply that the muon energy spectrum from real EAS is harder than that from simulated ones at a given primary energy.

Acknowledgements: One of the authors (J.C.A.V.) wants to thank the partial support from CONACYT (grant A1-S-46288) and the Consejo de la Investigación Científica de la Universidad Michoacana.

References

- [1] H.P.Dembinski et al., for the EAS-MSU, IceCube, KASCADE-Grande, NEVOD-DECOR, PierreAuger, SUGAR, Telescope Array, and Yakutsk EAS Array collaborations, arXiv:1902.08124v1 [astro-ph.HE].
- [2] S. Ostapchenko, *Phys. Rev. D* **83** (2011) 014018.
- [3] T. Pierog et al., *Phys. Rev. C* **92**, (2015) 034906.
- [4] F. Riehn et al., Proc. of the *34th ICRC*, PoS (ICRC2015) **558**.
- [5] W.D. Apel et al., *NIM A* **620** 202 (2010).
- [6] F. Riehn et al., Proc. of the *34th ICRC*, PoS (ICRC2017) **301**.
- [7] A.G. Bogdanov et al., *Phys. Atom. Nucl.* 73, 1852 (2010), *Yad. Fiz.* 73,1904(2010).
- [8] A.G. Bogdanov et al., *Astropart. Phys.* 98, 13 (2018).
- [9] J.A. Bellido et al., *Phys. Rev. D* 98, 023014 (2018).
- [10] T. Antoni et al., *NIM A* **513** (2003) 490.
- [11] D. Heck et al., Report No. FZKA 6019, Forschungszentrum Karlsruhe-Wissenschaft Berichte (1998).
- [12] A.Fasso et al., Report CERN-2005-10,INFN/TC-05/11, SLAC-R-773 (2005).
- [13] W.D. Apel et al., KASCADE-Grande Collaboration, *Astrop. Phys.* 36 (2012) 183.
- [14] W.D. Apel et al., KASCADE-Grande Collaboration, *Astrop. Phys.* 95 (2017) 25.
- [15] V. Verzi et al., Pierre Auger Collaboration, ICRC 2019, POS(ICRC2019) 450.
- [16] H.P. Dembinski et al., ICRC 2017, PoS (ICRC2017) 533.
- [17] R. Brun and F. Rademakers, *NIMA* 389 (1997) 81.
- [18] J.C. Arteaga-Velázquez et al. (KASCADE-Grande Collaboration), EPJ Web of Conferences 172, 07003 (2018).
- [19] W.D. Apel et al. , KASCADE-Grande Collaboration, *NIM A* 620 (2010) 202.

Full Authors List: KASCADE-Grande Collaboration

W.D. Apel^a, J.C. Arteaga-Velázquez^b, K. Bekk^a, M. Bertaina^c, J. Blümer^{a,d}, H. Bozdog^a, E. Cantoni^{c,f}, A. Chiavassa^c, F. Cossavella^d, K. Daumiller^a, V. de Souza^g, F. Di Piero^c, P. Doll^a, R. Engel^{a,d}, D. Fuhrmann^h, A. Gherghel-Lascu^e, H.J. Gils^a, R. Glasstetter^h, C. Grunpⁱ, A. Haungs^a, D. Heck^a, J.R. Hörandel^j, T. Huege^a, K.-H. Kampert^h, D. Kang^{a,*}, H.O. Klages^a, K. Link^a, P. Luczak^k, H.J. Mathes^a, H.J. Mayer^a, J. Milke^a, C. Morello^f, J. Oehlschläger^a, S. Ostapchenko^l, T. Pierog^a, H. Rebel^a, D. Rivera-Rangel^b, M. Roth^a, H. Schieler^a, S. Schoo^a, F.G. Schröder^a, O. Sima^m, G. Toma^e, G.C. Trinchero^f, H. Ulrich^a, A. Weindl^a, J. Wochele^a, J. Zabierowski^k

^a Karlsruhe Institute of Technology, Institute for Astroparticle Physics, Karlsruhe, Germany

^b Universidad Michoacana, Inst. Física y Matemáticas, Morelia, Mexico

^c Dipartimento di Fisica, Università degli Studi di Torino, Italy

^d Institut für Experimentelle Teilchenphysik KIT - Karlsruhe Institute of Technology, Germany

^e Horia Hulubei National Institute of Physics and Nuclear Engineering, Bucharest, Romania

^f Osservatorio Astrofisico di Torino, INAF Torino, Italy

^g Universidade São Paulo, Instituto de Física de São Carlos, Brasil

^h Fachbereich Physik, Universität Wuppertal, Germany

ⁱ Department of Physics, Siegen University, Germany

^j Dept. of Astrophysics, Radboud University Nijmegen, The Netherlands

^k National Centre for Nuclear Research, Department of Astrophysics, Lodz, Poland

^l Frankfurt Institute for Advanced Studies (FIAS), Frankfurt am Main, Germany

^m Department of Physics, University of Bucharest, Bucharest, Romania